

# **Electromechanical Bioreactor for Volumetric Muscle Loss Treatment**

A Technical Report submitted to the Department of Biomedical Engineering

Presented to the Faculty of the School of Engineering and Applied Science  
University of Virginia • Charlottesville, Virginia

In Partial Fulfillment of the Requirements for the Degree  
Bachelor of Science, School of Engineering

**Benedict Albergo**

Spring, 2022.

Technical Project Team Members

Curtis Creech

Aparna Kola

Caroline Roden

On my honor as a University Student, I have neither given nor received unauthorized aid on this assignment as defined by the Honor Guidelines for Thesis-Related Assignments

Steven Caliari, Department of Biomedical Engineering

# Electromechanical Bioreactor for Volumetric Muscle Loss Treatment

Benedict Albergo<sup>a,1</sup>, Curtis Creech<sup>b</sup>, Aparna Kola<sup>c</sup>, Caroline Roden<sup>d</sup>

<sup>a-d</sup> Undergraduate student, University of Virginia

<sup>1</sup> Correspondence: ba9mm@virginia.edu, University of Virginia, 516-375-3617

## **Abstract**

Biomaterials-based methods to treat volumetric muscle loss are lacking in their ability to treat combined nerve and muscle damage. An anisotropically aligned and electrically conductive tissue engineered scaffold for growing skeletal muscle was recently developed for the purpose of addressing this gap in the field. Using bioreactor preconditioning on these scaffolds during myocyte and nerve cell incubation may encourage improved myogenesis and neural growth in seeded cells. To this end, a novel bioreactor was created capable of both electrically and mechanically stimulating these preexisting scaffolds. The bioreactor produced accommodates five scaffolds and will provide tunable uniaxial strain as well as direct electrical stimulation to each scaffold. Strain analysis confirms that the scaffold is receiving the intended strain as programmed into the bioreactor controls. Electrical stimulation will be delivered via electrodes directly inserted into each scaffold, and voltage output will be confirmed with voltmeter measurements. By designing a novel bioreactor that can precondition skeletal muscle scaffolds, further strides may be made in understanding and treating combined nerve and muscle damage associated with volumetric muscle loss.

Keywords: volumetric muscle loss, scaffold, bioreactor, electromechanical

---

## **Introduction**

Volumetric muscle loss (VML) is a broad term used to describe permanent, large-scale damage to muscle tissue that results in some form of decreased function<sup>1,2</sup>. It is extremely common in military settings, as a recent study found that among 14,500 military personnel evacuated from battlefields between 2001 and 2013, 77% reported musculoskeletal injuries<sup>3</sup>. Civilian populations are also affected by VML with approximately 250,000 new cases of open fractures per year in the US<sup>4</sup>. Traditional approaches to treat VML have limited effectiveness, as muscle grafts require large volumes of tissue which can lead to donor site morbidity<sup>5,6</sup>. Additionally, most approaches do not account for the frequent comorbidity of VML with damage to nerve tissue<sup>7,8</sup>. As such, functional repair of VML is difficult to achieve with traditional methods.

Biomaterials-based approaches have been attempted in recent years, but most are only effective at treating simple injuries<sup>7,9</sup>. Since muscle function is highly dependent on innervation and a strong connection at the neuromuscular junction (NMJ), the Caliri lab has developed a new scaffold for regenerating skeletal muscle to address these needs. The collagen-glycosaminoglycan polypyrrole (CG-PPy) scaffold is three dimensional, anisotropically aligned,

and electrically conductive<sup>10</sup>. The goal of this scaffold is to encourage myogenic cells to mature and proliferate according to these spatial and environmental cues to regenerate VML/NMJ injuries. Many past studies have indicated the beneficial effects of mechanical or electrical stimulation on tissue development. For engineered skeletal muscle constructs, these include an improvement in cell alignment, differentiation, and contractility following in vivo implantation<sup>11,12</sup>. However, the synergistic use of electromechanical stimulation to drive myogenic maturation has not been widely explored. This study aimed to develop an electromechanical bioreactor system to promote myogenesis of existing CG-PPy scaffolds seeded with muscle derived cells (MDCs). To produce a functional prototype, we sought to (1) design and fabricate a bioreactor system capable of providing cyclic electrical pulsation and uniaxial tensile loading to the seeded scaffolds and (2) test bioreactor efficacy and tuning of electrical and mechanical stimulation.

## Results

### Design Considerations

To construct a bioreactor capable of housing and cyclically stimulating myogenic cells for extended time periods within an incubator, many important considerations had to be taken. Main considerations included the sterility of the internal chamber, tunability of components for adjustment and sterilization, stability of dynamic components, and ease of use. From a less technical perspective, basic user experience considerations were also taken into account, namely ease of use to run the bioreactor protocol. These fabrication features and user criteria of the bioreactor prototype are summarized in **Table 1**.

Design Constraint	Fabrication Features
Sterility	Use of biocompatible materials (e.g. biomed amber resin, stainless steel) inside chamber
	Minimization of entry holes for electrical and mechanical components
	Rounded geometries for ease of sterilization
	Bending of rods (as opposed to welding) to conserve anticorrosive properties of stainless steel
	Clamp crossbar at lower depth than rod entry to prevent media leakage
Tunability	Threading of rods to allow for adjustable screw connection of rods; threading of crossbar for convenient tensile clamp attachment
	Expansion of inner chamber to allow for mechanical system assembly/adjustment
	Coupled stepper motor-potentiometer system to fine-tune voltage for electrical stimulation
Stability	Use of ball bearing flanges to guide linear motion
	Motor mount to reduce stress on bioreactor chamber
Ease of use	Use of switching circuit to mitigate corrosion in media bath
	Stand-alone bioreactor design with no need for computer connection
	Touchscreen display used for easy input process

**Table 1.** Summary of considerations for bioreactor design.

### Electrical and Mechanical Hardware Assembly

The functioning prototype of the bioreactor including the electronics system is seen in **Figure 1**. More specifically, the bioreactor chamber and its mechanical and electrical hardware components are seen in **Figure 2**. To achieve linear actuation, a rod system was fabricated that is driven by a stepper motor equipped with a threaded shaft and lead screw (**Figure 3**). Dual L-shaped rods connect a crossbar in the chamber with a rod tree that acts as an external linkage for the lead screw. The crossbar includes attachment threads

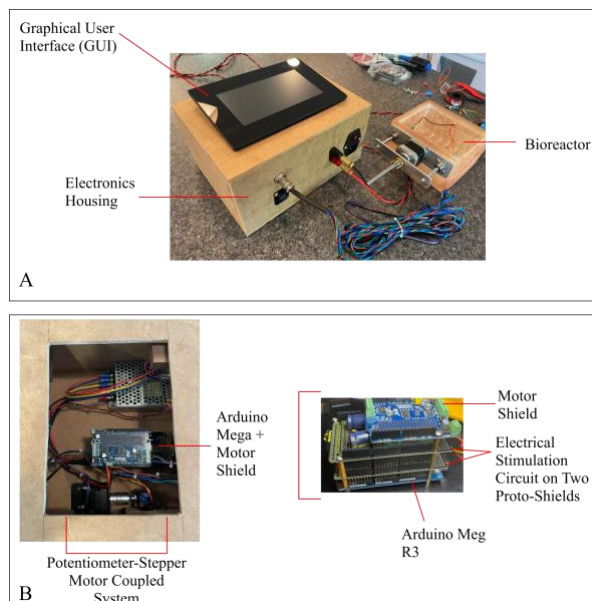


**Figure 1.** Labelling of Bioreactor System Layout (A) and Electronics for Reference (B).

for five tensile clamps. Electrically, a network of ten electrodes, two per scaffold, connects to each terminal of the scaffolds and enters the inner chamber via a dome cap cable gland. Clamps, shown in **Figure 2**, attach to the crossbar and static attachment sites via stainless steel screws and matching nut attachments.

The electrical circuit, shown in **Figure 4**, uses a DC-DC up converter run through a motorized potentiometer to provide 1.27 to 55VDC to the electrodes. The potentiometer forms

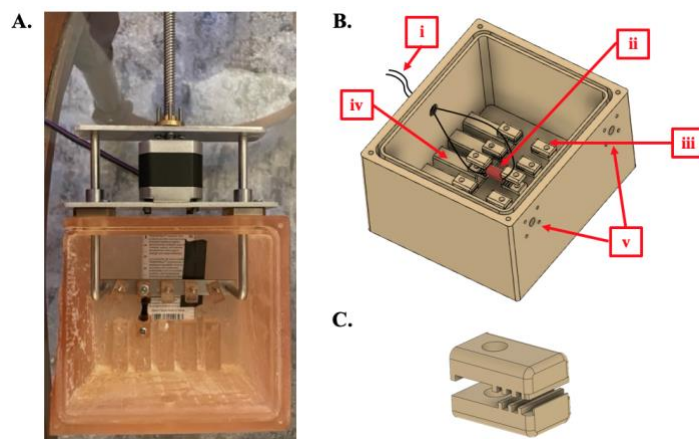


**Figure 2.** Overview of Bioreactor Design. (A) Fabricated bioreactor assembly. (B) Bioreactor base and electrode/clamp assembly. Five pairs of electrodes (one pair shown for representation) (i) attach to the terminals of each scaffold (ii) gripped by tensile clamps (iii). Clamp attachment columns (iv) allow for the fixation of static clamps. The holes shown on the base (v) acts as entry points for rods and thread holes for linear bearing attachment. (C) Scaled-up view of tensile clamp design.

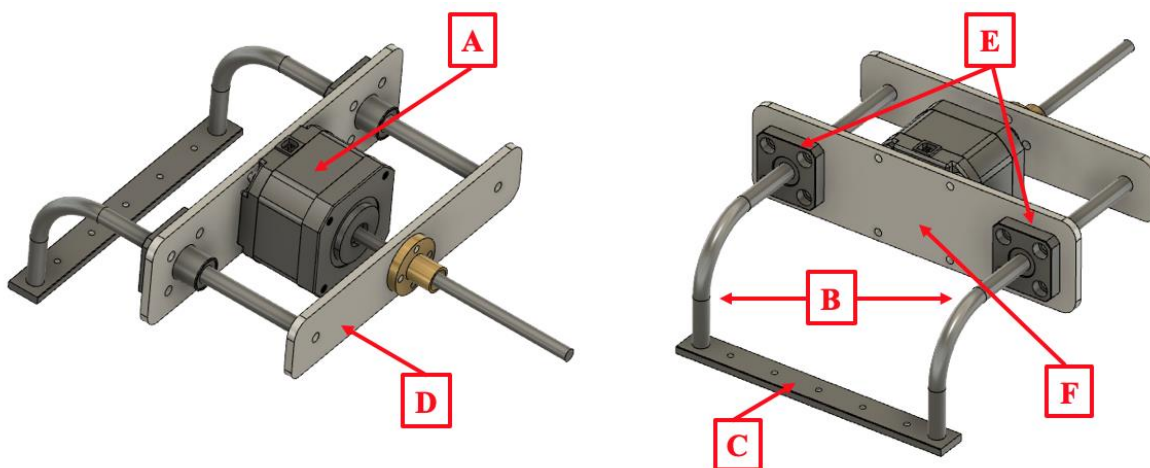


**Figure 3. Mechanical Rod System for Linear Actuation.** A stepper motor with a threaded shaft and lead screw (A) linearly moves dual L-shaped rods (B) that connect to the tensile clamp attachment crossbar (C). The rods and lead screw connect externally at a rod tree (D). Linear bearings (E) that attach to the bioreactor base provide stability for actuation and a linkage point for the stepper motor mount (F).

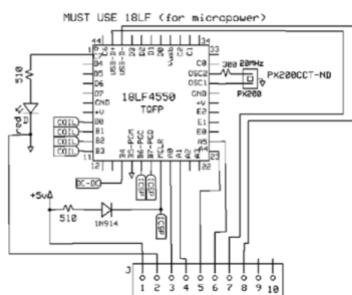
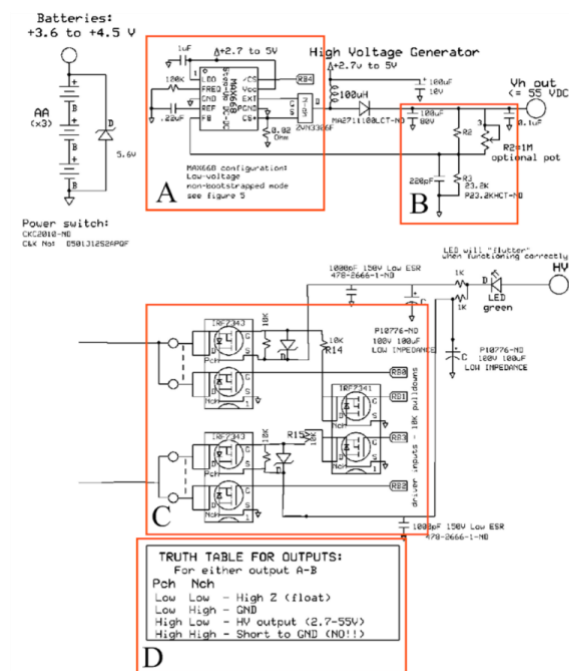


**Figure 4. Diagram of Electrical Circuit.** (A) DC-DC Buck Converter (B) Stepper motor controls potentiometer which adjusts electrical stimulation input voltage (C) Switching circuit which mitigates electrode corrosion in bioreactor media bath.

Replace resistor network with 1M equivalents for 2.7V micropower operation

Orthopedic TVEMV Pulse Gen.		
Ortho-TVEMF-2008-a		
RG Dennis	Rev. C 7/17/2008	1

a voltage divider with a 22k Ohm resistor. The output of the voltage divider is kept constant by the DC-DC converter by a reference voltage on the feedback pin of 1.25VDC. Keeping the output of the voltage divider constant, but varying the input resistor by way of a potentiometer causes the voltage at the input of the voltage divider to be amplified and output to the electrodes. The electrodes are fed through a switching circuit consisting of three transistors to allow switching of electrode polarity. Alternating positive electrodes mitigates electrode corrosion caused by voltage differences while in the media bath. The DC-DC up converter is switched on and controlled by the Arduino

Mega microprocessor, as is activation of the switching circuit's transistors to alternate electrically positive and ground electrodes. Voltage to the CG-PPy scaffold is applied based upon the following equation:

$$V_{out} = V_{ref} \cdot \left( \frac{R_2}{R_3} + 1 \right) \quad [1]$$

where  $V_{ref}$  is 1.25 VDC,  $R_2$  is a  $1M\Omega$  linear taper potentiometer, and  $R_3$  is a fixed resistor at  $22k\Omega$ . The  $1M\Omega$  potentiometer will be is coupled to a 200-step motor controlled by the Arduino through a motor driver board. This allows precise adjustment of the high voltage output to

the scaffold from 1.47 - 58 VDC in 140 mVDC steps. The Arduino will also control the low voltage circuit, capable of providing 0 - 3.3VDC in 13mVDC steps through a voltage divider with an Arduino programmable AD5242 256 step digital potentiometer.

Stepper motors are run by an AdaFruit Stepper Motor Driver V2. The motor driver and Arduino Mega are powered by an AC-DC converter that provides 5V to the Arduino and 12V to the motor driver board. An LCD touchscreen provides standalone capability while maintaining end user programming of the electromechanical stimulation variables such as frequency and duration. No desktop or laptop computer is needed to program stimulation, though a USB port permits the end user to customize the software as needed.

### Graphical User Interface Design

Based on user criteria to easily run and monitor the bioreactor protocol, the Graphical User Interface (GUI) was implemented on a 7-inch touchscreen display integrated into the electrical housing of the product (**Figure 1**). The GUI is the primary method by which the user inputs electrical and mechanical stimulation values to run the bioreactor, starts and stops the bioreactor protocol, and monitors an experiment (**Figure 5**). Specifically, inputs common to the electrical and mechanical stimulation include total runtime which sets how many hours the bioreactor will be run, total pulse duration which sets the duration of the pulse train in minutes, pulse duration which sets the length of each pulse in seconds within the minute, and pulse frequency (Hz) which defines how many pulses there are in a second (**Figure 5F**). The amplitude of the pulse is defined by a voltage input for electric stimulation, and a strain (%) input for mechanical stimulation. The display defaults to a menu page from which the user navigates to one of four pages 1) the electrical stimulation setup page 2) the mechanical stimulation setup page 3) the start page 4) and the stop page. On the 'input/setup' pages, the user can input values using the touchscreen sliders. The 'start' page is used to initiate electromechanical stimulation in the bioreactor, and monitor the time elapsed in seconds, minutes, and hours since the beginning of stimulation to aid in data collection. The 'stop' page terminates the stimulation protocol by stopping the running code and confirms this event to the user.

### Uniaxial Strain Assessment to Validate Mechanical Assembly

To validate the accuracy of linear actuation, the stimulation of hydrated CG-PPy scaffolds were imaged in real time to



**Figure 5: Graphical User Interface (GUI) Panels (A) Menu page for navigating display (B) Electrical value input page (C) Mechanical value input page (D) Bioreactor start and monitoring page (E) Bioreactor stop page (F) Graphical representation of electrical and mechanical stimulation input values**

analyze the displacement resulting from uniaxial strain. In different trials, the displacement of 10mm scaffolds were measured at 10% (1 mm), 20% (2 mm), and 30% (3 mm) strain. Although this approach aims to apply 10% strain to the current scaffold size, higher strain percentages were measured to assess mechanical system accuracy if larger scale constructs were used in the future. Displacement measurements were taken at the interface between the scaffold and the clamp in motion at different loci along the y-axis of the scaffold to ensure accurate strain throughout the construct. Specifically, displacement values were computed at 2 mm, 4 mm, and 6 mm from the bottom base of the scaffold. Image J analysis was performed to compare the observed and expected displacement at each strain percentage and loci (**Figure 6**). Three one-tailed t-tests determined no significant differences between observed and expected displacement values at each strain percentage ( $p_{1,2,3} < 0.01$ ), confirming accuracy of strain. It is important to note that displacement values were taken at a fixed point on the x-axis, thus a comparison of strain at different x-axis loci must be completed in the future to verify accurate stimulation throughout the scaffold.

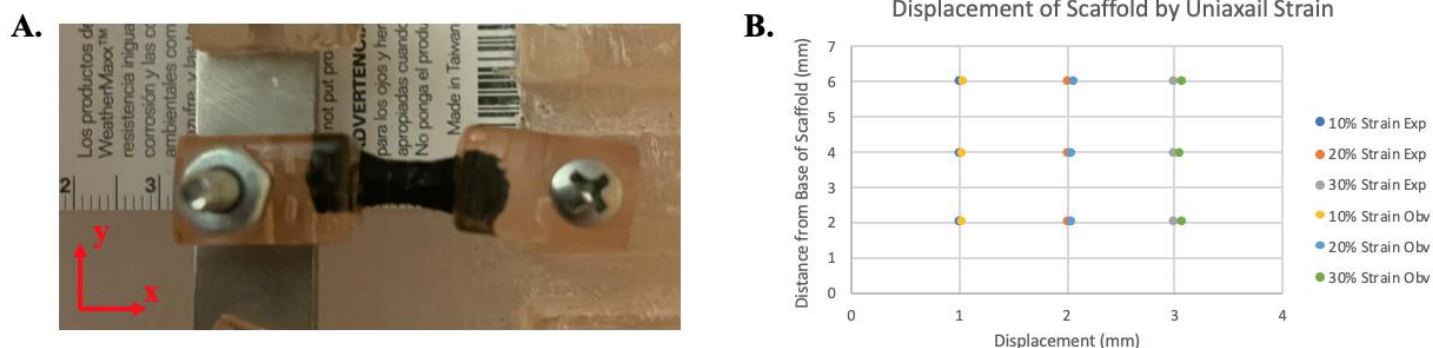


**Figure 6. Validation of Linear Actuation via Strain Displacement Analysis.** (A) Real time image of scaffold stimulation in 10% strain trial. Axes of scaffold are specified for analysis. (B) Observed vs. expected displacement of 10 mm scaffolds at 10%, 20%, and 30% strain at 2 mm, 4 mm, and 6 mm from bottom base of scaffold in y-axis. Displacement measurements from loci in y-axis computed from interface of scaffold and left dynamic clamp. Three one tailed t-tests of observed vs. expected displacement values at 10% ( $p_1$ ), 20% ( $p_2$ ), and 30% ( $p_3$ ) strain at a 5% alpha level showed no significant difference between populations ( $p_1 = 2.780E-03$ ,  $p_2 = 2.828E-03$ ,  $p_3 = 6.880E-05$ ).

### General Bioreactor User Protocol

1. Sterilize bioreactor
  - a. Expose entire bioreactor under UV radiation for 15 minutes
  - b. Further sterilize bioreactor by spraying isopropyl alcohol into corners and interfaces (e.g. screw, rod, clamp interfaces) of bioreactor
2. Configure and calibrate bioreactor
  - a. Physically zero the mechanical and electrical systems
    - i. Pull lead screw into starting position
    - ii. Check that circuit is closed with voltmeter
3. Scaffold placement
  - a. Gather four hydrated CG-PPy scaffolds
  - b. Use sterilized tweezers to insert one side of scaffold into far-end side clamp
  - c. Secure scaffold in clamp by screwing clamp
  - d. Repeat steps 3.a-c for each of the four scaffolds on each set of far-end side clamps
  - e. Bring the actuator-attached clamp rod close to the unattached end of the scaffold
  - f. Secure each scaffold to the near-end side clamps one at a time and secure them by screwing down clamps one at a time
4. Input stimulation values into GUI display
  - a. From the menu page, navigate to ‘electrical’ under ‘inputs/setup’
    - b. Input the desired values and return to the ‘menu’
    - c. From the menu page, navigate to ‘mechanical’ under ‘inputs/setup’
    - d. Input the desired values and return to the ‘menu’
5. Run the programmed electromechanical stimulation protocol
  - a. Upload the Arduino code
  - b. Press ‘start’ under ‘control’ on the GUI

### Discussion

A novel bioreactor was produced for the purposes of stimulating skeletal muscle scaffolds both electrically and mechanically. Though delays in the electrical stimulation circuit have resulted in it being unfinished, the necessary steps to finish this aspect of the design are well-defined and will be completed following delivery of necessary materials. Design substitutions must occur before cell testing can commence, however the current product can mechanically stimulate unseeded scaffolds to the desired specifications. This bioreactor will be able to hold five scaffolds at once, maintain cell culture, and reside in an incubator for the duration of scaffold preconditioning. A graphical user interface was produced to allow easy control of the device from outside an incubator.

Limitations of this project lie with access to materials and fabrication methods. Many biocompatible materials are significantly more expensive than standard materials, and are more difficult to obtain due to supply-chain constraints. One such limitation revolves around the fabrication of the bioreactor body. The ideal method for manufacturing would be to obtain a solid block of PTFE and machine out the inside to the desired shape. However, this subtractive manufacturing was inaccessible with respect to the time constraints of this project design. As such, an extrusion-

based 3D printing method was chosen, with a tradeoff of error in printing and expensive resin materials. Additionally, the optimal metals for the parts inside the reactor (i.e., crossbar, L-rods) would be medical-grade stainless steel. The stainless steel used has the same fabrication process as it would for the medical-grade material, so a material substitution down the line would be convenient for future researchers. A key change that will need to be made in future iterations is the substitution of platinum wiring for the current copper electrodes currently in place. Platinum wiring is cytocompatible, making it an ideal material for direct electrical stimulation of each scaffold. It is, however, significantly more expensive than copper, and is better suited for a final iteration, as it also has the same physical properties as the current design and can be easily substituted for the copper wire. Due to supply chain limitations, initial DC-DC up converters were obtained in used condition from an Ebay seller and, unfortunately, were defective. New converters were procured from Newark Electronics and can easily be replaced in the network.

Initial next steps to complete the assembly of the bioreactor system include the fabrication of a top hatch to seal the inner chamber equipped with filters for carbon dioxide and heat exchange within the incubator. Additionally, a printed circuit board will need to be designed to replace through-hole breadboard prototypes to form a permanent connection for soldered electrical components. In the long term, the effect of electromechanical stimulation on myoblast proliferation and maturation will be tested in the completed bioreactor system. Following cyclic stimulation, the alignment and organization of actin and myosin using immunofluorescence will be measured and compared to static culture to assess myogenesis.

## **Materials and Methods**

### ***Bioreactor Chamber and Tensile Clamps***

Autodesk Fusion 360 was used to design the bioreactor chamber and clamps. These parts were then printed from FormLabs BioMed Amber Resin using a FormLabs Form 2 SLA printer at the Architecture School at UVA. Printed components proceeded to be washed in isopropyl alcohol for ten minutes using a FormWash and cured at 60°C for 30 minutes in a FormCure. 3D printed supports were removed using an oscillating multitool blade. The bioreactor was then sanded to remove any final unwanted material.

### ***Mechanical Rod System***

Static components of the mechanical rod system were purchased from McMaster Carr and fabricated at UVA's

Lacy Hall. An Iverntech NEMA 17 Stepper Motor with Integrated 100mm T8 Lead Screw was acquired from Amazon. The crossbar was fabricated from 440C stainless steel. The rod tree and motor mount were constructed from 6061 aluminum and fabricated via a water cutter. The mechanical rods, also made from 440C stainless steel, were bent at 90° using a bending machine and threaded at both ends with a lathe and drill tap to allow their screw attachments to the crossbar and rod tree. The crossbar was threaded at clamp connection points using a manually operated drill tap. Following machine fabrication, the individual parts were connected via 6-32 stainless steel Phillip's head screws.

### ***Electrode and Linear Actuator Motor Electrical Network***

A set of ten 22 AWG copper electrodes were custom made from wire obtained from Amazon. They are run from a distribution block connected to electrode leads connected via soldered quick disconnects to the electrical box's electrode output, which utilizes a simple speaker five way binding post. The linear actuator motor mounted on the bioreactor is connected via four wires using a Molex connector to a four-wire aircraft XLR microphone port on the electrical box. These connectors allow easy disconnect from both the bioreactor in the cell culture incubator and the main electrical box, while preventing any possible error connecting the wires together. The Arduino Mega and AdaFruit Motor Driver V2 boards were obtained via Amazon.

### ***Electrical Circuit***

The DC-DC converter utilizes a MAX668EUB+ sourced from Newark Electronics. The potentiometer is a 1MΩ linear taper, 2W version obtained from DigiKey. The switching network uses two IRF7343 dual N and P channels and one IRF7341 dual N channel MOSFET transistors. The transistors and DC-DC converter are surface mounts designed to be used on printed circuit boards. To convert them for easy prototyping via breadboards, they were soldered onto SMD to DIP conversion boards. Other various electrical parts such as capacitors, resistors, diodes and inductors, see **Figure 3**, were obtained via DigiKey, Mouser Electronics, and Amazon. The components were soldered in place on two Arduino Mega protoshield boards obtained from Ebay to allow for easy stacking and compact circuit design.

### ***Arduino Code for Electromechanical Control***

The Arduino code uses finite state machines to turn the mechanical and electrical stimulation circuits on or off in

synchrony or independently, depending on end user input obtained via the LCD touchscreen GUI. In addition to mechanical strain and electrical voltage, the end user can control the duration of each stimulation and their frequencies. Duration consists of stimulation trains in seconds, durations in minutes, and total run time in hours. Due to memory limitations inherent to the Arduino microprocessor boards, total runtime cannot exceed 15 days without program time being automatically reset. Commented code with details on usage can be found on the project Github:

<https://github.com/prnakla/BioreactorArduinoCode.git>.

### ***Graphical User Interface***

The Graphical User Interface (GUI) is implemented using a Nextion 7" LCD touchscreen display (Figure 1). The Nextion software is used to compile a Text Formatter Plus Text Information (TFT) file uploaded to the display using a FAT32 SD card. The buttons and input sliders on the display are registered and assigned to an action in the Arduino software. The buttons and input sliders are assigned to an id number, which is used in the arduino code for electromechanical control to translate input values to the designated electrical or mechanical stimulation event.

### ***Uniaxial Strain Analysis***

To hydrate unseeded CG-PPy scaffolds, constructs were immersed in 100% ethanol for 1 h followed by soaking in PBS for 12 h. Stimulation of scaffolds was imaged using an iPhone 12 Pro. Displacement of scaffolds was measured using ImageJ using a scale bar inserted into the inner chamber of the bioreactor.

### **End Matter**

#### ***Author Contributions and Notes***

B.A. and C.R. primarily focused on mechanical system fabrication and clamp/base components while C.C and A.K. primarily developed and built the electromechanical circuit, Arduino code, and GUI.

#### ***Acknowledgments***

We would like to acknowledge the following individuals for their guidance throughout the design project: Project Advisors – Steven Caliarì, Ivan Basurto; Fabrication Advisors – Sebring Smith, Trevor Kemp, Dwight Dart; Capstone Advisors – Shannon Barker, Timothy Allen, Vignesh Valaboju, Noah Perry; Additional Support – Michael Rariden, John Link.

### **References**

1. Machingal, M. A. et al. A tissue-engineered muscle repair construct for functional restoration of an irrecoverable muscle injury in a murine model. *Tissue Eng. Part A* 17, 2291–2303 (2011).
2. Corona, B. T. et al. Further development of a tissue engineered muscle repair construct in vitro for enhanced functional recovery following implantation in vivo in a murine model of volumetric muscle loss injury. *Tissue Eng. Part A* 18, 1213–1228 (2012).
3. Belmont, P. J. et al. The nature and incidence of musculoskeletal combat wounds in Iraq and Afghanistan (2005-2009). *J. Orthop. Trauma* 27, e107-113 (2013).
4. Meling, T., Harboe, K. & Søreide, K. Incidence of traumatic long-bone fractures requiring in-hospital management: a prospective age- and gender-specific analysis of 4890 fractures. *Injury* 40, 1212–1219 (2009).
5. Corona, B. T., Rivera, J. C., Owens, J. G., Wenke, J. C. & Rathbone, C. R. Volumetric muscle loss leads to permanent disability following extremity trauma. *J. Rehabil. Res. Dev.* 52, 785–792 (2015).
6. Sarrafian, T. L., Bodine, S. C., Murphy, B., Grayson, J. K. & Stover, S. M. Extracellular matrix scaffolds for treatment of large volume muscle injuries: A review. *Vet. Surg.* 47, 524–535 (2018).
7. Gilbert-Honick, J. & Grayson, W. Vascularized and innervated skeletal muscle tissue engineering. *Adv. Healthc. Mater.* 9, 1900626 (2020).
8. Yang, P. J. & Temenoff, J. S. Engineering orthopedic tissue interfaces. *Tissue Eng. Part B Rev.* 15, 127–141 (2009).
9. Owens, B. D. et al. Combat wounds in operation Iraqi Freedom and operation Enduring Freedom. *J. Trauma* 64, 295–299 (2008).
10. Basurto, I. M., Mora, M. T., Gardner, G. M., Christ, G. J. & Caliarì, S. R. Aligned and electrically conductive 3D collagen scaffolds for skeletal muscle tissue engineering. *Biomaterial. Sci.* 9, 4040–4053 (2021).
11. Moon, D. G., Christ, G., Stitzel, J. D., Atala, A. & Yoo, J. J. Cyclic mechanical preconditioning improves engineered muscle contraction. *Tissue Eng. Part A* 14, 473–482 (2008).
12. Ko, U. H. et al. Promotion of Myogenic Maturation by Timely Application of Electric Field Along the



Topographical Alignment. *Tissue Eng. Part A* 24,  
752–760 (2018).